Role of GAP-43 in Sequestering Phosphatidylinositol 4,5-Bisphosphate to Raft Bilayers

Jihong Tong,* Lam Nguyen,* Adriana Vidal,* Sidney A. Simon,†‡ J. H. Pate Skene,† and Thomas J. McIntosh*

*Department of Cell Biology, †Department of Neurobiology, and ‡Center of Neuroengineering, Duke University Medical Center, Durham, North Carolina

ABSTRACT The lipid phosphatidylinositol 4,5-bisphosphate (PIP_2) is critical for a number of physiological functions, and its presence in membrane microdomains (rafts) appears to be important for several of these spatially localized events. However, lipids like PIP_2 that contain polyunsaturated hydrocarbon chains are usually excluded from rafts, which are enriched in phospholipids (such as sphingomyelin) containing saturated or monounsaturated chains. Here we tested a mechanism by which multivalent PIP_2 molecules could be transferred into rafts through electrostatic interactions with polybasic cytoplasmic proteins, such as GAP-43, which bind to rafts via their acylated N-termini. We analyzed the interactions between lipid membranes containing raft microdomains and a peptide (GAP-43P) containing the linked N-terminus and the basic effector domain of GAP-43. In the absence or presence of nonacylated GAP-43P, PIP_2 was found primarily in detergent-soluble membranes thought to correspond to nonraft microdomains. However, when GAP-43P was acylated by palmitoyl coenzyme A, both the peptide and PIP_2 were greatly enriched in detergent-resistant membranes that correspond to rafts; acylation of GAP-43P changed the free energy of transfer of PIP_2 from detergent-soluble membranes to detergent-resistant membranes by -1.3 kcal/mol. Confocal microscopy of intact giant unilamellar vesicles verified that in the absence of GAP-43P PIP_2 was in nonraft microdomains, whereas acylated GAP-43P laterally sequestered PIP_2 into rafts. These data indicate that sequestration of PIP_2 to raft microdomains could involve interactions with acylated basic proteins such as GAP-43.

INTRODUCTION

Membrane microdomains (''rafts'') are thought to play critical roles in a variety of biological functions such as signal transduction (1–6), cytoskeletal organization (7–9), lipid sorting (10,11), and protein trafficking/recycling (12–14). The composition of membrane rafts is often characterized by analysis of detergent-resistant membranes (DRMs) that are obtained by detergent extraction at 4°C (15–20). DRMs have been found to be enriched in cholesterol and sphingolipids such as sphingomyelin (SM) that primarily have saturated hydrocarbon chains, whereas detergent-soluble membranes (DSMs) are enriched in membrane phospholipids, such as phosphatidylcholine (PC), that contain unsaturated hydrocarbon chains (15,21,22). In addition, several classes of proteins are enriched in DRMs, including acylated cytoplasmic proteins (4,19,23).

A key lipid component of rafts is phosphatidylinositol 4,5-bisphosphate (PIP_2), which is critical to a number of important cell functions such as production of second messengers (24–26), enzyme activation (27), regulation of potassium and transient receptor potential (TRP) channels (28–31), membrane trafficking (27,32,33), and regulation of the actin cytoskeleton (7–9,34). The presence of PIP_2 in rafts appears to be critical in a number of these spatially localized membrane functions (7–9,26,32,35), although it is important to note that not all PIP_2 is localized in rafts (36). Considering only its polyunsaturated hydrocarbon chain composition, one might expect PIP_2 to be preferentially localized in nonraft bilayers, as rafts are composed primarily of cholesterol and phospholipids containing saturated and monounsaturated hydrocarbon chains. That is, as noted by Shaw et al. (37), based on partitioning experiments with lipids of different hydrocarbon chain compositions (38,39) it seems likely that the four double bonds typically found in the *sn*-2 hydrocarbon chain of PIP_2 would make it energetically unfavorable for PIP_2 to reside in cholesterol-enriched raft domains as compared to nonraft domains.

PIP_2 has been shown (7,27,37,40–43) to strongly bind to several cytoplasmic proteins, such as myristoylated alanine-rich protein kinase C substrate (MARCKS), cortical associated protein of 23 kDa (CAP-23), neural axonal myristoylated protein of 22 kDa (NAP-22), and growth associated protein of 43 kDa (GAP-43). These proteins all contain clusters of basic amino acid residues, often called ''basic effector domains'' (7,27,40–43). In bilayers containing a single lipid domain, it has been shown that peptides containing such basic effector domains laterally sequester PIP_2 in the plane of the bilayer, even in the presence of larger concentrations of monovalent negatively charged phospholipids such as phosphatidylglycerol or phosphatidylserine (40–43). GAP-43 is of special interest since it is an abundant raft-associated protein in developing and regenerating neurons and is involved in the development of axons and nerve growth cones (44,45), in nerve regeneration after injury (46,47), and in the regulation

Submitted April 10, 2007, and accepted for publication August 27, 2007.

Address reprint requests to Thomas J. McIntosh, E-mail: t.mcintosh@cellbio.duke.edu.

Editor: Lukas K. Tamm.

0006-3495/08/01/125/09 $2.00

doi: 10.1529/biophysj.107.110536

of neurotransmitter release (48). Moreover, it has been shown that GAP-43 associates with rafts due to dual palmitoylation of its N-terminus (48,49).

In this article we experimentally test the hypothesis that upon acylation GAP-43 transfers PIP_2 from nonraft into raft microdomains. For these experiments we use detergent extraction procedures to determine quantitatively the localization of PIP_2 in DRMs and DSMs extracted from bilayers containing microdomains. We also use confocal microscopy to determine the location of fluorescently labeled PIP_2 in raft and nonraft microdomains in intact vesicles of the same lipid compositions. We measure the interactions of these bilayers with a peptide (GAP-43P) that contains both the N-terminus and basic effector domains of GAP-43. The N-terminus of GAP-43P contains two cysteine residues that can be acylated with palmitoyl coenzyme A. Before and after palmitoylation of GAP-43P, we quantitatively determine the distribution in DRMs and DSMs of both PIP_2 and peptide, and calculate the free energy of transfer of PIP_2 between these domains in the presence and absence of peptide.

MATERIALS AND METHODS

Materials

1,2-Dioleoyl-*sn*-glycero-3-phosphocholine (DOPC), 1,2-dioleoyl-*sn*-glycero-3-[phospho-*rac*-(1-glycerol)] (DOPG), sphingomyelin (SM), cholesterol (Chol), *n*-palmitoyl-sphingosine-1-succinyl (methoxy (polyethylene glycol))-2000 (PEG-Cer), phosphatidylinositol 4,5-biphosphate (PIP_2), and palmitoyl coenzyme A (CoA) were purchased from Avanti Polar Lipids (Alabaster, AL). Phosphatidylinositol 4,5-biphosphate (myo-inositol-2-^{3}H(N)) (tritiated PIP_2) was obtained from American Radiolabeled Chemicals (St. Louis, MO). For confocal microscopy experiments, red fluorescently labeled PIP_2 (BODIPY TMR-PIP_2-C16) and the green lipid fluorescent marker 3,3′-dilinoleoyloxacarbocyanine perchlorate (DiO) were purchased from Echelon Research Laboratories (Salt Lake City, UT) and Molecular Probes (Eugene, OR), respectively. All lipids were used without further purification.

Phosphorus standard solution and silica gel coated thin layer chromatography plates were purchased from Sigma-Aldrich (St. Louis, MO). The 32-amino-residue peptide Ac-MLCCMRRTKQAHKAATKIQASFRGHITRKKLK-NH_2 was synthesized and purified by Bachem California (Torrance, CA). This peptide, which we refer to as GAP-43P, is a fusion of two functionally important regions of GAP-43. Residues 1–10 of the peptide correspond to the N-terminus (membrane binding site) of GAP-43, which contains two cysteine residues known to be acylated in vivo (48,49). The next 22 residues of the peptide correspond to the protein's basic effector domain (residues 31–52 in human GAP-43), containing the PIP_2 binding activity. The 2-D Quant kit for peptide assay was purchased from Amersham Biosciences (Piscataway, NJ).

Preparation of sucrose-loaded large unilamellar vesicles

Large unilamellar vesicles (LUVs) were prepared by standard procedures as follows. The appropriate lipids were codissolved in chloroform:methanol (2:1 v/v). Our standard lipid mixtures were DOPC/DOPG/SM/Chol (30:10:30:30, molar ratio) or DOPC/DOPG/SM/Chol/PIP_2 (30:10:30:30:1), both with 10-wt% PEG-Cer added to prevent aggregation of the LUVs. After the solvent was removed by rotary evaporation, the dry lipid film was hydrated with 48 mM sucrose in 50 mM Tris buffer, pH 8.0, with five freeze-thaw cycles. The resulting dispersions, at concentrations of 15–20 mg/ml, were extruded 11 times through two stacked polycarbonate filters with pore size of 100 nm to form LUVs. The sucrose solution on the outside of the LUVs was removed by first diluting five times with an isoosmotic buffer (25 mM KCl in 50 mM Tris buffer, pH 8.0), centrifuging at 115,000 $\times$ g at 10°C for 1 h, and then resuspending the pellets with an appropriate amount of 25 mM KCl, 50 mM Tris, pH 8.0, buffer (50). The phospholipid content of the LUVs was determined by phosphate assay (51).

GAP-43 peptide binding

The binding to LUVs of either unacylated or acylated GAP-43P was performed with an initial lipid/peptide molar ratio of 50:1 using a centrifugation procedure (50). For the case of unacylated peptide, GAP-43P was mixed with sucrose-loaded LUVs in 25 mM KCl, 50 mM Tris buffer, pH 8.0, and incubated at room temperature for 1 h. In separate experiments, GAP-43P was acylated (palmitoylated) using similar procedures to those described by Quesnel and Silvius (52) by mixing palmitoyl CoA and GAP-43P at a 5:1 molar ratio and incubating with the LUV suspension at 37°C for 1 h. For experiments in either the presence of absence of palmitoyl CoA, bound peptide was separated from unbound peptide by ultracentrifugation for 1 h at 115,000 $\times$ g at 10°C. The supernatant (containing unbound peptide) and the pellet (containing LUVs and bound peptide) were collected and the pellet was resuspended in 25 mM KCl, 50 mM Tris buffer, pH 8.0. For both the supernatant and pellet the phospholipid content was determined by phosphate analysis and GAP-43P concentration was analyzed with the 2-D Quant assay. For each assay appropriate standard curves were run for GAP-43P in buffer or in buffer with palmitoyl CoA, with the reaction time for the last step of the assay being the same for each standard curve and sample analysis.

After the incubation of GAP-43P with palmitoyl CoA and LUVs, mass spectrometry was used to verify that the GAP-43P had indeed been palmitoylated. All samples were run on an Applied Biosystems (Foster City, CA) Voyager DE-Pro that was calibrated in linear mode immediately before acquiring the sample spectra. The accelerating voltage was 20,000 volts, the delay time was 100 ns, and the scan range was 500–4000 Da. The matrix used was a saturated solution of 4-hydroxy-alpha-cyano-cinnamic acid purchased from Sigma-Aldrich (MALDI-MS grade). Samples were mixed with the matrix in a ratio of 1:3 and a 1.2 μL aliquot of the solution was spotted on the plate and allowed to dry. A nitrogen laser was light fired onto the spot. All spectra were averages of a minimum of three spectra summed to provide better mass accuracy. In the absence of palmitoyl CoA, spectra of GAP-43P in solution with or without added LUVs displayed a sharp peak at a mass of 3783 Da, corresponding to the expected molecular weight of the peptide. In the presence of palmitoyl CoA an additional large sharp peak was observed at a mass of 4263 Da, corresponding to a doubly palmitoylated GAP-43P. Other smaller peaks were recorded at 4041, 4551, and 4788 Da, corresponding to the peptide containing one, three, or four palmitates. Doubly palmitoylated peptide would be expected since this peptide has two cysteines near the N-terminus and Quesnel and Silvius (52) showed that cysteine residues are palmitoylated by this procedure. Peptides with one palmitate indicate peptides with incomplete acylation of their cysteines, whereas the peptides with three or four palmitates could possibly correspond to additional acylation of lysine residues, as lysines near or within a cluster of basic residues could have a lowered pKa and might also be acylated (Dr. John Silvius, personal communication, 2006).

Detergent extraction and chemical analysis of DRMs and DSMs

Detergent extraction experiments were conducted as follows: LUVs with or without bound GAP-43P were treated with 1% Triton X-100 for 30 min at 4°C and then centrifuged at 15,000 $\times$ g for 1 h at 4°C. The supernatant was removed and collected, and the pellets were resuspended with an equal volume of buffer and then vortexed. For both the supernatant (containing

detergent-soluble membranes or DSMs) and the resuspended pellets (containing detergent-resistant membranes or DRMs) the phospholipid contents were determined by phosphate assay (51) and the peptide concentrations were analyzed using the 2-D Quant assay. We (53) have previously used both wide-angle and low-angle x-ray diffraction analysis to demonstrate that DRMs prepared in this way are both liquid and more ordered than the DSMs from this lipid system. For each 2-D Quant assay, appropriate standard curves were run for GAP-43P in buffer, in buffer with palmitoyl CoA, in buffer with 1% Triton X-100, or in buffer with palmitoyl CoA and 1% Triton X-100.

To estimate the distribution of DOPC, DOPG, and SM in DSMs and DRMs, thin layer chromatography (TLC) was employed with the solvent chloroform/methanol/ammonium hydroxide 65:25:4 (v:v:v). The DSMs and DRMs were lyophilized, dissolved in the TLC solvent, and loaded onto the TLC plates so that each lane contained the same amount of total phospholipid. Iodine vapor was used to detect the lipid and peptide spots, with control lanes containing only DOPC, DOPG, SM, or GAP-43P identifying the relative positions of these components. The relative intensities of the peaks in TIFF images of the plates were determined by measuring peak areas with NIH Image Version 1.61.

To determine the distribution of PIP_2 in the DRMs and DSMs, 0.1% tritiated PIP_2 was added to the appropriate lipid mixtures. After GAP-43P binding and detergent extraction, we employed a Packard (Meriden, CT) Tri-Carb 2100TR liquid scintillation analyzer to determine the radioactivity of the tritiated PIP_2 in the DRMs and DSMs. Usually 10–15 μL of each sample was added into 3 mL of the high flash point cocktail Safety-Solve scintillation solution (Research Products International, Mount Prospect, IL.) and measured with the scintillation counter.

Calculations of molar partition coefficients and apparent free energies of transfer

The mol-fraction partition coefficient for GAP-43P from DSM to DRM was calculated from

$$K_p = ([G]_R/[G]_S)\times(([L]_S + [G]_S)/[L]_R + [G]_R)), \quad (1)$$

where $[G]_R$ and $[G]_S$ represent the molar concentrations of GAP-43P in the DRM and DSM phase, respectively, and $[L]_R$ and $[L]_S$ are the molar concentrations of total lipid (phospholipid plus cholesterol) in the DRM and DSM phase, respectively. The phospholipid content in DRMs and DSMs was determined by phosphate assay (51) and the cholesterol content was calculated based on our previous measurements of cholesterol/total lipid (0.2 for DSMs and 0.4 for DRMs) for similar lipid systems (54). The mol-fraction partition coefficient for PIP_2 from DSM to DRM was calculated from

$$K_p = ([PIP_2]_R/[PIP_2]_S)\times([L]_S)/[L]_R), \quad (2)$$

where $[PIP_2]_R$ and $[PIP_2]_S$ represent the molar concentrations of PIP_2 in the DRM and DSM phase, respectively. The apparent free energies of transfer from DSMs to DRMs were obtained using

$$\Delta G_a = -RT \ln (K_p), \quad (3)$$

where R is the molar gas constant and T is temperature in degrees Kelvin. The thermal energy (RT) is 0.55 kcal/mol at 277 °K (4°C). An implicit extra thermodynamic assumption of these calculations is that the presence of 1% Triton X-100 does not alter the distribution (or K_p) of the lipids or peptides between DSMs and DRMs. We therefore refer to the energies as apparent free energies (ΔG_a).

Confocal microscopy

Confocal microscopy was used to determine the distribution of BODIPY TMR-labeled PIP_2 in intact raft-containing giant unilamellar vesicles (GUVs) in the presence and absence of GAP-43P. GUVs were made following the procedures of Akashi et al. (55) with slight modifications. Small amounts (typically <1 mol %) of BODIPY TMR-PIP_2 and DiO were added to DOPC/DOPG/SM/Chol/PEG-ceramide in chloroform/methanol. These chloroform/methanol solutions were deposited on a roughened Teflon surface and allowed to dry under vacuum; 100 mM sucrose was then added at 37°C and incubated for 2–3 h. The resulting lipid cloud that detached from the Teflon plate contained GUVs. This lipid cloud was carefully collected in plastic tubes and prepared for microscopy by diluting with 100 mM glucose (external solution), placing on a microscope slide, and then covering with a glass coverslip. Since the inside of the vesicles contained sucrose and the outside contained the lower density glucose, the GUVs sank to the microscope slide.

The GUVs were observed with a 63× NA 1.4 Plan Apochromat oil objective on a LSM 510 Meta Zeiss (Jena, Germany) confocal microscope. Configurations for double channel excitation and the choice of emission of the fluorochromes were made to prevent cross talk and the two colors were scanned using multitrack line switching. The green DiO lipid labels were observed with the use of a 488-nm filter, whereas the red-labeled BODIPY TMR-PIP_2 was visualized with a 543-nm filter. Quantification of lipid probe colocalization was performed with the Zeiss LSM AIM 3.2 enhanced colocalization software that permitted the determination of the number of green and red pixels in each region of the bilayer. To determine if the proportion of DiO and BODIPY TMR-PIP_2 pixels were significantly different in the observed bilayer microdomains, we employed a sample test for equality of proportions without continuity correction using the χ-square test ($\alpha = 0.05\%$) (56,57).

RESULTS

Peptide binding

Fig. 1 shows the percentage of nonacylated and acylated GAP-43P bound to DOPC/DOPG/SM/Chol LUVs in the presence or absence of PIP_2. The addition of 1% PIP_2 to these bilayers caused no significant change in GAP-43P binding. However, acylation of GAP-43P produced a large increase in binding. For example, in the absence of PIP_2 only 43% GAP-43P bound to DOPC/DOPG/SM/Chol bilayers,

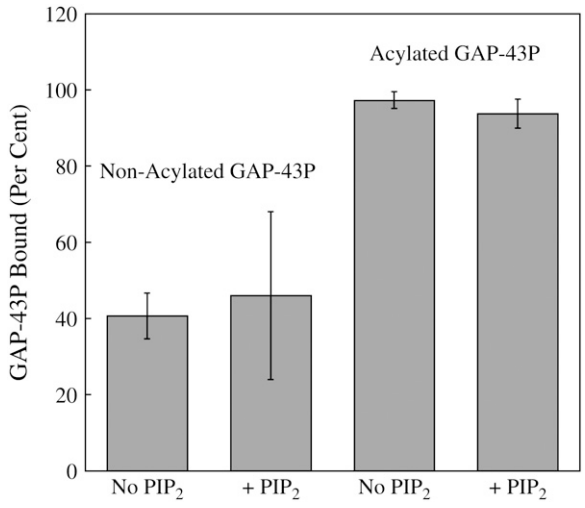

FIGURE 1 Percentage of acylated or nonacylated GAP-43P bound to LUVs containing 30:10:30:30 DOPC/DOPG/SM/Chol or 30:10:30:30:1 DOPC/DOPG/SM/Chol/PIP_2. Each bar indicates mean ± SD for three to five experiments.

whereas 97% of acylated GAP-43P bound to bilayers of that composition.

Distribution of phospholipids, GAP-43P, and PIP_2 between DRMs and DSMs

After detergent extraction, phosphate analysis showed that for all the tested systems the total phospholipids were more or less equally distributed between the DSMs and DRMs (Fig. 2). Thin layer chromatography (Fig. 3) was used to determine the distributions of DOPC, DOPG, and SM in DSMs and DSMs obtained from three DOPC/DOPG/SM/Chol preparations: 1), with no GAP-43P, 2), with non-acylated GAP-43P, and 3), with acylated GAP-43P. For each system SM was enriched in the DRMs, whereas DOPC and DOPG were enriched in the DSMs (Fig. 3 and Table 1). In addition, the presence of GAP-43P could be observed at the origin of the relevant TLC lanes. Nonacylated GAP-43P was preferentially observed in DSMs, whereas acylated GAP-43P was enriched in DRMs (Fig. 3; Table 1).

2D Quant analysis of the distribution of GAP-43P in DSMs and DRMs (Fig. 4) showed quantitatively that the acylation of GAP-43P had a marked effect on the distribution of the peptide in DSMs and DRMs. In the presence or absence of PIP_2 the ratio of GAP-43P in DRMs to DSMs increased upon GAP-43P acylation (Fig. 4). For example, in the absence of PIP_2 the DRM/DSM ratio of GAP-43P increased from <1 to >5.

Experiments with tritiated PIP_2 (Fig. 5) showed that, either in the absence or in the presence of nonacylated GAP-43P, PIP_2 was enriched in DSMs compared to DRMs. That is, when normalized to the total phospholipid (PL) in each component, the PIP_2/PL ratio was $\sim$0.5 for DRMs compared to DSMs. However, in the presence of acylated GAP-43P the

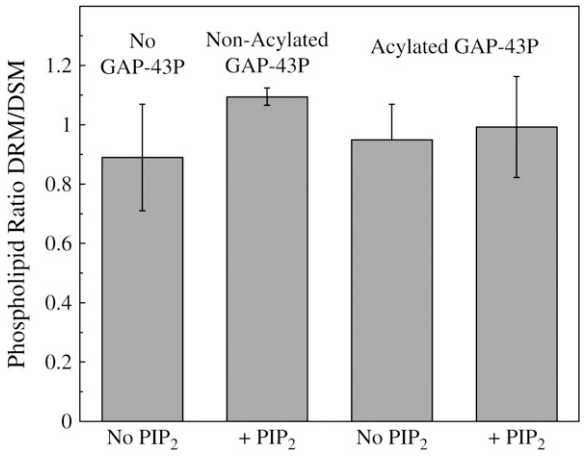

FIGURE 2 The phospholipid ratio in DRMs/DSMs extracted from LUVs containing 30:10:30:30 DOPC/DOPG/SM/Chol or 30:10:30:30:1 DOPC/DOPG/SM/Chol/PIP_2 in the absence GAP-43P, in the presence of non-acylated GAP-43P, or in the presence of acylated GAP-43P. Each bar indicates mean $\pm$ SD for three to five experiments.

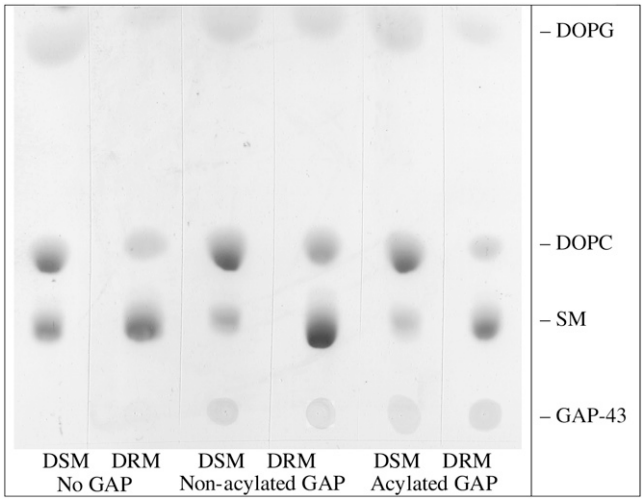

FIGURE 3 Thin layer chromatogram of DRMs and DSMs from 30:10:30:30 DOPC/DOPG/SM/Chol in the absence GAP-43P, in the presence of non-acylated GAP-43P, or in the presence of acylated GAP-43P.

PIP_2 was highly enriched in DRMs compared to DSMs, so that the PIP_2/PL ratio was $\sim$6.5 for DRMs compared to DSMs (Fig. 5).

Apparent free energies of transfer of GAP-43P or PIP_2 from DSMs to DRMs

With the assumption that the Triton X-100 does not change the composition of bilayer DRMs, the peptide and PIP_2 distributions can be put on a thermodynamic basis by calculations of the molar partition coefficients (K_p) and apparent free energies of transfer (ΔG_a) from DSMs to DRMs. Table 2 presents the molar partition coefficients (K_p) and the apparent free energies of transfer (ΔG_a) for GAP-43P and PIP_2 from DSMs to DRMs. In either the presence or absence of nonacylated peptide, ΔG_a for PIP_2 was about $+0.5$ kcal/mol, indicating that it was energetically favorable for this lipid to be in DSMs. For nonacylated GAP-43P, ΔG_a was also positive, $+0.33$ kcal/mol in the absence of PIP_2 and $+0.21$ kcal/mol in the presence of PIP_2, indicating that it was also energetically favorable for the nonacylated peptide to be associated with DSMs. However, when GAP-43P was acylated, the free energies of transfer of either peptide or PIP_2 were negative, indicating that under these conditions it was energetically favorable for these molecules to be in DRMs. For example, the binding of palmitoylated GAP-43P to

TABLE 1 Density ratios (DRM/DSM) of spots in TLC

Molecule	No GAP-43P	Nonacylated GAP-43P	Acylated GAP-43P
DOPC	0.34 $\pm$ 0.06	0.52 $\pm$ 0.14	0.28 $\pm$ 0.12
DOPG	0.35 $\pm$ 0.07	0.49 $\pm$ 0.19	0.29 $\pm$ 0.04
SM	1.90 $\pm$ 0.52	2.87 $\pm$ 1.15	2.10 $\pm$ 0.04
GAP-43P	–	0.78 $\pm$ 0.44	1.40 $\pm$ 0.58

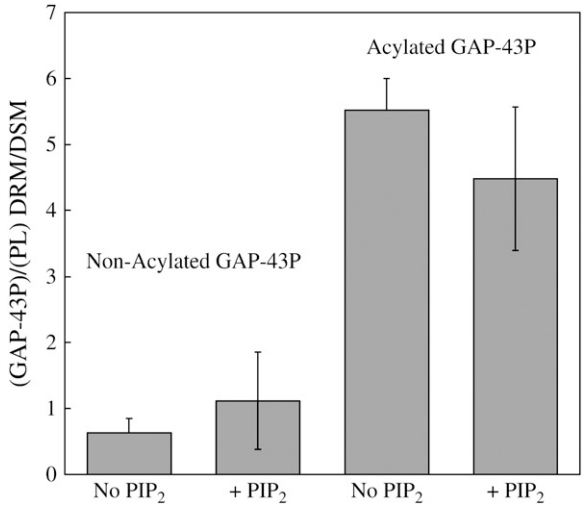

FIGURE 4 Distribution of nonacylated or acylated GAP-43P in DRMs and DSMs extracted from 30:10:30:30 DOPC/DOPG/SM/Chol or 30:10:30:30:1 DOPC/DOPG/SM/Chol/PIP_2 LUVs. Each bar indicates mean ± SD for three to five experiments.

DOPC/DOPG/SM/Chol/PIP_2 bilayers changed the free energy of transfer of PIP_2 from DSMs to DRMs from +0.45 kcal/mol to −0.87 kcal/mol.

Confocal microscopy

Fig. 6 shows confocal images of equatorial slices of GUVs containing the green fluorescent lipid DiO and the red fluorescently labeled PIP_2. The top row of Fig. 6 shows a typical GUV in the absence of GAP-43P. The red BODIPY TMR-PIP_2 was colocalized with the green lipid marker DiO

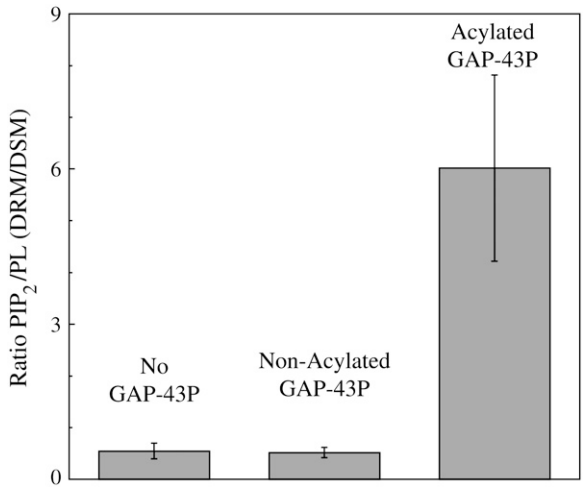

FIGURE 5 Distribution of radio-labeled PIP_2 between DRMs and DSMs in the absence GAP-43P, in the presence of nonacylated GAP-43P, or in the presence of acylated GAP-43P. Each bar indicates mean ± SD for three to five experiments.

TABLE 2 Partition coefficients (K_p) and apparent free energies of transfer (ΔG_a) of PIP2 and GAP-43P from DSMs to DRMs

Molecule	PIP_2 present	GAP-43P present	K_p	ΔG_a (kcal/mol)
PIP_2	Yes	No	0.44 ± 0.06	+0.45 ± 0.08
PIP_2	Yes	Nonacylated	0.41 ± 0.08	+0.49 ± 0.12
GAP-43P	No	Nonacylated	0.56 ± 0.16	+0.33 ± 0.16
GAP-43P	Yes	Nonacylated	0.68 ± 0.62	+0.21 ± 0.47
PIP_2	Yes	Acylated	5.0 ± 1.4	−0.87 ± 0.16
GAP-43P	No	Acylated	4.4 ± 0.4	−0.81 ± 0.05
GAP-43P	Yes	Acylated	3.6 ± 0.8	−0.70 ± 0.11

Values represent either mean ± SD for three to five experiments. For comparison, thermal energy is 0.55 kcal/mol.

in a large microdomain (labeled *1*) in the left-hand side of the GUV. As shown in Table 3, for this particular vesicle >99% of both the red and green pixels were localized in this microdomain 1, with <1% of the pixels in the nonlabeled microdomain (domain *2*). This colocalization analysis was also performed on six other GUVs in the absence of GAP-43, with each showing >99% colocalization of red and green pixels. Because the unsaturated DiO preferentially localizes to nonraft microdomains (58,59), these images indicate that, in the absence of peptide, BODIPY TMR-PIP_2 was enriched in nonraft (green-containing) membranes. This observation was consistent with the data showing that, in the absence of GAP-43P, PIP_2 was found preferentially in DSMs (Fig. 5).

The addition of acylated GAP-43P changed the distribution of the lipids in the GUVs (Fig. 6, *bottom row*). In the presence of acylated GAP-43P, much smaller microdomains containing green and/or red probes were observed (Fig. 6, *bottom row*). To quantitate the overlap of green and red probes we divided the equatorial section in Fig. 6 into 13 small regions and measured the green (DiO) and red (TMR-PIP_2) pixels in each region. As can be seen in Table 3, regions 2, 7, 9, and 11 contained mostly green pixels, regions 1, 4, and 6 contained mostly red pixels, whereas regions 3, 5, 8, 10, 12, and 13 contained roughly equal amounts of green and red pixels. Thus, the presence of acylated GAP-43P removed much of the TMR-PIP_2 from the green nonraft bilayers. A sample test for equality of proportions was used testing the null hypothesis that the red and green markers had the same distribution among the regions. The *p*-values were between 0.4 and 1.0 for regions 3, 8, 12, and 13, but were $<2.2 \times 10^{-16}$ for regions 1, 2, 4, 6, and 7, with intermediate *p*-values for the other regions. Similar results and *p*-values were obtained with five other vesicles from similar preparations. Thus, compared to the control vesicles (Fig. 6, *top*), the introduction of acylated GAP-43P significantly changed the distribution of TMR-PIP_2 relative to the nonraft marker DiO.

DISCUSSION

Several water-soluble cytoplasmic proteins, including the protein kinase C substrates MARCKS, CAP-23, and GAP-43, contain clusters of positively charged amino acids that bind the membrane lipid PIP_2 (27,40,42). In our studies we

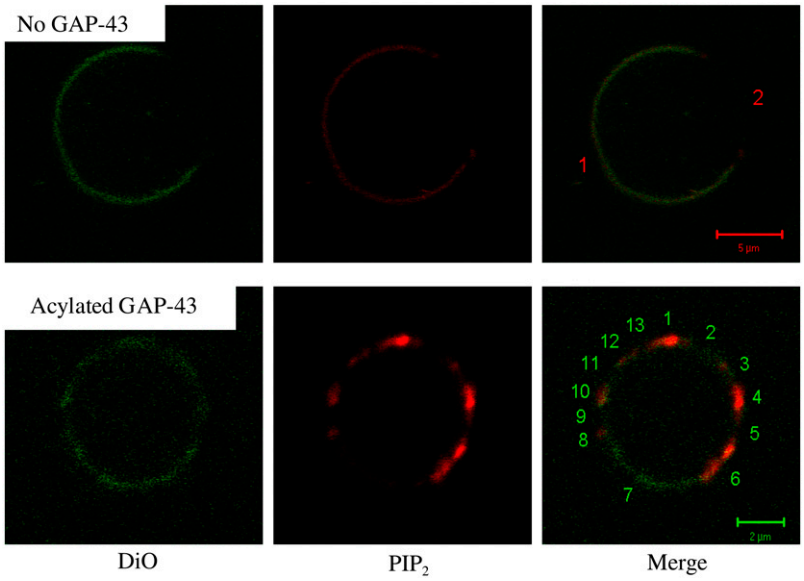

FIGURE 6 Confocal images of 30:10:30:30 DOPC/DOPG/SM/Chol GUVs containing fluorescently labeled DiO and PIP_2. The top row shows a vesicle in the absence of GAP-43P with filters showing the green DiO (*left*), the red BODIPY TMR-PIP_2 (*middle*), and a dual-colored merged image (*right*). The bottom row shows a vesicle in the presence of acylated GAP-43P with filters showing the green DiO (*left*), the red PIP2 (*middle*), and a merged image (*right*). For each vesicle, microdomains are numbered in the right image.

have examined the interactions with lipid bilayers of a 32-amino-acid peptide (GAP-43P) corresponding to the N-terminus domain linked to the basic effector domain of GAP-43. Quantitative analyses of the distribution of GAP-43P and PIP_2 were performed with detergent extraction experiments, which have been extensively used to study the composition of microdomains in both cell membranes and lipid bilayers (15–17,23,26,59–63). Previous x-ray diffraction experiments (53) have analyzed the structure of the DRMs and DSMs from the bilayer system used in this study. However, detergents partition into and break apart bilayers, potentially modifying lipid-lipid interactions (36,60,64,65). Therefore, to verify and supplement the detergent extraction results, we also used confocal microscopic observations of intact vesicles of the same lipid compositions (59).

Previous studies have shown that a peptide corresponding to the effector domain of GAP-43 (without the N-terminus) binds to LUVs containing negatively charged lipids (40). This binding of the effector domain was shown to be due to nonspecific electrostatic interactions (40). Our experiments with GAP-43P, containing both the N-terminus and the effector domain, showed that acylation significantly increased peptide binding to LUVs containing negatively charged lipids to the extent that virtually all of the peptide was bound (Fig. 1).

TABLE 3 Pixel distributions in regions of GUVs

Without GAP-43P													
Pixel color	Region 1												Region 2
Green	1574												10
Red	1737												3
With acylated GAP-43P													
Pixel color	1	2	3	4	5	6	7	8	9	10	11	12	13
Green	204	126	112	107	48	239	553	54	32	135	43	90	19
Red	532	6	113	545	86	844	8	63	3	242	1	98	13

See Fig. 6.

The acylation of GAP-43P markedly increased the concentration of both the peptide (Fig. 4) and PIP_2 (Fig. 5) in DRMs compared to DSMs. That is, the acylation of GAP-43P changed the apparent free energy of transfer of PIP_2 from DSMs to DRMs (Table 2) from $\Delta G_a = +0.45$ kcal/mol to $\Delta G_a = -0.87$ kcal/mol. This energy difference of 1.32 kcal/mol is significantly larger than thermal energy (0.55 kcal/mol), suggesting that electrostatic interactions between PIP_2 and acylated positively charged proteins such as GAP-43 could have a significant impact on the sequestering of PIP_2 into membrane rafts.

The binding of either acylated or nonacylated GAP-43P had little effect on the amount of DSMs or DRMs extracted with detergent (Fig. 2). The observation that the peptide did not markedly change the distribution of monovalent DOPG between DRMs and DSMs (Fig. 3; Table 1) is consistent with the observations of Golebiewska et al. (43) that showed that peptides with clusters of basic residues do not sequester monovalent acidic phospholipids such as phosphatidylglycerol.

In the absence of GAP-43P, PIP_2 was preferentially extracted in DSMs (Fig. 5) and BODIPY TMR-PIP_2 was preferentially localized in large nonraft microdomains in intact vesicles (Fig. 6; Table 3). Thus, in the absence of GAP-43P the detergent extraction and confocal experiments were in complete agreement indicating that PIP_2 prefers nonraft to raft microdomains. In the case of native PIP_2 this is expected given that one of its hydrocarbon chains is polyunsaturated. The location of both native PIP_2 and BODIPY TMR-PIP_2 in nonraft domains is also consistent with the results of Gambhir et al. (41) who observed that both lipids are excluded from cholesterol-enriched domains in monolayers. Moreover, the amount of phospholipid was similar in DRMs and DSMs (Fig. 2) and the relative sizes of the nonraft

and raft domains were approximately equal as viewed in intact vesicles (typical vesicle is shown in Fig. 6). Therefore, in the absence of peptide the detergent extraction appears to provide a valid representation of the bilayer microdomain composition.

In the presence of acylated GAP-43P the detergent extraction and confocal experiments were in agreement in that they both indicated that the acylated peptide modified the distribution of PIP_2 in the plane of the bilayer. Several of the observed 13 equatorial regions (Fig. 6, *bottom*) contained mostly green pixels, as expected for nonraft bilayers not containing red BODIPY TMR-PIP_2, whereas other regions contained mostly red pixels corresponding to BODIPY TMR-PIP_2 in raft bilayers (Table 3). Other regions contained a mixture of green and red pixels, corresponding to the presence of BODIPY TMR-PIP_2 in nonraft bilayers. Thus, the confocal experiments confirm that acylated GAP-43P targets at least some of the PIP_2 away from nonraft bilayers into rafts. However, in comparing the detergent extraction and confocal experiments there are three factors to consider. First, during detergent extraction GAP-43P had access to both sides of the bilayer, whereas in the confocal experiments the added peptide presumably had access to only the outer lipid monolayer of the intact GUV, explaining why GUVs exposed to GAP-43P contained regions with both green and red pixels (Table 3). Second, because the fluorescently labeled PIP_2 contains the BODIPY moiety in its hydrocarbon chain region, its partitioning properties could be somewhat different than unlabeled PIP_2. Third, although the detergent extraction method indicated that the DRMs and DSMs contained similar amounts of lipid (Fig. 2), it provided no information on the lateral dimensions of the microdomains. The confocal images indicated that the raft and nonraft microdomains were of smaller lateral dimensions in the presence of acylated GAP-43P. Shaw et al. (37) previously observed that myristoylated NAP-22 broke up raft domains in a similar ternary lipid system.

Our results are summarized in diagrammatic form in Fig. 7. In the absence of peptide, DRMs and DSMs had different compositions; DRMs were enriched in SM (with its mostly saturated hydrocarbon chains) and cholesterol, whereas DSMs were enriched in the unsaturated lipids DOPC, DOPG, and PIP_2. We found that palmitoylated GAP-43P bound primarily to DRMs, as do a variety of acylated membrane proteins (4,19,23). The effector domain of GAP-43P bound PIP_2 and therefore sequestered this lipid to DRMs (Fig. 7 *B*).

In a recent study Golebiewska et al. (43) present an intriguing model whereby proteins with clusters of basic residues, such as MARCKS, can nucleate raft lipids. In this model proteins with interfacial phenylalanines that penetrate into the interfacial region increase local lateral surface pressure and decrease the local thickness of the lipid monolayer, thereby attracting lipids with small polar headgroups, such as cholesterol. Our experiments indicate that preformed raft microdomains can sequester acylated proteins such as GAP-43.

For several cell lines, Laux et al. (7) showed that GAP-43 is extracted in DRMs and in intact cells colocalizes with PIP_2 in plasma membrane microdomains. They also showed that the binding of PIP_2 and its effects on cell actin dynamics depend on the effector domain of GAP-43. Our results point to the importance of GAP-43 diacylation in colocalizing the protein and PIP_2 in the raft microdomains. That is, in terms of sequestering PIP_2 to rafts, these experiments demonstrate the importance of both the effector domain and the acylated N-terminus of GAP-43. As a corollary, we propose that some of the cellular PIP_2 not localized to raft microdomains in cells (36) could represent PIP_2 that is not bound to acylated proteins such as GAP-43.

Once in a raft, the PIP_2 would be in close physical proximity to raft-localized actin binding proteins and signaling proteins. Since it seems likely that a given molecule of PIP_2 could not bind to GAP-43 and to another protein at the same time, the PIP_2 would have to be released from GAP-43

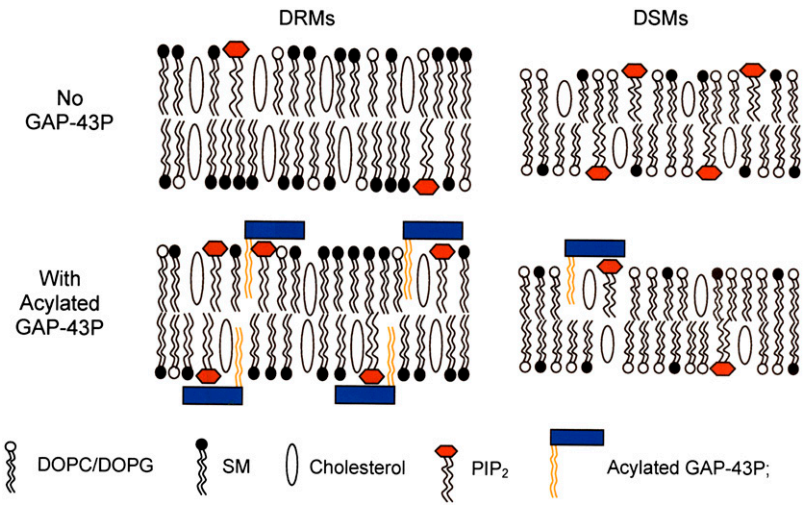

FIGURE 7 Schematic diagrams showing the distribution of PIP_2 in DRMs and DSMs in the absence (*top row*) and presence (*bottom row*) of acylated GAP-43P. In the absence of GAP-43P (*top*) the PIP_2 is primarily located in DSMs along with the other unsaturated lipids DOPC and DOPG, whereas the DRMs are enriched in SM and cholesterol. When acylated GAP-43P is added (*bottom*), the peptide binds and preferentially sequesters the PIP_2 into the raft microdomains (DRMs). Note that during detergent extraction procedures the GAP-43P gains access to both sides of the bilayer.

to participate in classical PIP_2 signaling pathways. This would mean that the availability of PIP_2 for signaling would be a function of the off-rate of PIP_2 from GAP-43 as well as the diffusion rate of free PIP_2 out of the raft microdomain. As a result PIP_2 would be transiently available at high concentrations only to signaling molecules that are themselves highly concentrated within the raft. Therefore it seems possible that PIP_2 released from GAP-43 would be in a position to interact with concentrated signaling proteins before diffusing out of the raft. As PIP_2 diffuses, it could rebind to another GAP-43 molecule, bind to phospholipase C (PLC), or partition into the surrounding nonraft microdomain. An important implication of these findings is that both the concentration of PIP_2 in raft domains, and the dynamics of its release for signaling, could be regulated by other signals that modify the affinity of the GAP-43 effector domain for PIP_2. The effector domain of GAP-43 binds apocalmodulin with higher affinity than calcium-calmodulin (66,67) and also contains a site for PKC phosphorylation (45). Therefore the binding of apocalmodulin would compete with PIP_2 binding to the effector domain and PKC phosphorylation would reduce binding of either calmodulin or PIP_2. Although the specific consequences for signal transduction remain to be elucidated, our findings suggest that in raft domains GAP-43-mediated concentration of PIP_2 would allow the availability of PIP_2 for signaling that would be modulated dynamically by calcium and PKC. Once the PIP_2 is hydrolyzed, the resulting diacyl glycerol should rapidly diffuse out of the raft into the surrounding bilayer.

In summary, we have demonstrated a mechanism by which PIP_2 can be sequestered into lipid rafts. The mechanism involves electrostatic binding of PIP_2 to proteins, such as GAP-43, that have effector domains containing clusters of positively charged amino acids. We argue that, when GAP-43 is acylated by cellular enzymes, the diacylated GAP-43 and its bound PIP_2, preferentially partition into raft microdomains.

We thank Dr. George Dubay, Department of Chemistry, Duke University, for performing the mass spectroscopy analysis and Dr. Tim Oliver of the Department of Cell Biology, Duke University Medical Center, for assistance with the confocal experiments.

This work was supported by National Institutes of Health grant GM27278 and by grants from Philip Morris Inc. USA and Philip Morris International.

REFERENCES

1. Simons, K., and D. Toomre. 2000. Lipid rafts and signal transduction. *Nat. Rev. Mol. Cell Biol.* 1:31–39.
2. Field, K. A., D. Holowka, and B. Baird. 1997. Compartmentalized activation of the high affinity immunoglubulin E receptor within membrane domains. *J. Biol. Chem.* 272:4276–4280.
3. Baird, B., E. D. Sheets, and D. Holowka. 1999. How does the plasma membrane participate in cellular signaling by receptors for immunoglobulin E? *Biophys. Chem.* 82:109–119.
4. Moffett, S., D. A. Brown, and M. E. Linder. 2000. Lipid-dependent targeting of G proteins into rafts. *J. Biol. Chem.* 275:2191–2198.
5. Pierchala, B. A., J. Milbrandt, and E. M. Johnson, Jr. 2006. Glial cell line-derived neurotrophic factor-dependent recruitment of Ret into lipid rafts enhances signaling by partitioning Ret from proteasome-dependent degradation. *J. Neurosci.* 26:2777–2787.
6. Young, R. M., X. Zheng, D. Holowka, and B. Baird. 2005. Reconstitution of regulated phosphorylation of FcepsilonRI by a lipid raft-excluded protein-tyrosine phosphatase. *J. Biol. Chem.* 280:1230–1235.
7. Laux, T., K. Fukami, M. Thelen, T. Golub, D. Frey, and P. Caroni. 2000. GAP43, MARCKS, and CAP23 modulate PI(4,5)P(2) at plasmalemmal rafts, and regulate cell cortex actin dynamics through a common mechanism. *J. Biol. Chem.* 149:1455–1472.
8. Caroni, P. 2001. New EMBO members' review: actin cytoskeleton regulation through modulation of PI(4,5)P(2) rafts. *EMBO J.* 20:4332–4336.
9. Kwik, J., S. Boyle, D. Fooksman, L. Margolis, M. P. Sheetz, and M. Edidin. 2003. Membrane cholesterol, lateral mobility, and the phosphatidylinositol 4,5-bisphosphate-dependent organization of cell actin. *Proc. Natl. Acad. Sci. USA.* 100:13964–13969.
10. Simons, K., and E. Ikonen. 2000. How cells handle cholesterol. *Science.* 290:1721–1726.
11. Brown, R. E. 1998. Sphingolipid organization in biomembranes: what physical studies of model membranes reveal. *J. Cell Sci.* 111:1–9.
12. Simons, K., and E. Ikonen. 1997. Functional rafts in cell membranes. *Nature.* 387:569–572.
13. Sharma, D. K., A. Choudhury, R. D. Singh, C. L. Wheatley, D. L. Marks, and R. E. Pagano. 2003. Glycosphingolipids internalized via caveolar-related endocytosis rapidly merge with the clathrin pathway in early endosomes and form microdomains for recycling. *J. Biol. Chem.* 278:7564–7572.
14. Ikonen, E. 2001. Roles of lipid rafts in membrane transport. *Curr. Opin. Cell Biol.* 13:470–477.
15. Hanada, K., M. Nishijima, Y. Akamatsu, and R. E. Pagano. 1995. Both sphingolipids and cholesterol participate in the detergent insolubility of alkaline-phosphatase, a glycosylphosphatidylinositol-anchored protein, in mammalian membranes. *J. Biol. Chem.* 270:6254–6260.
16. Ahmed, S. N., D. A. Brown, and E. London. 1997. On the origin of sphingolipid/cholesterol-rich detergent-insoluble cell membranes: physiological concentrations of cholesterol and sphingolipid induce formation of a detergent-insoluble, liquid-ordered lipid phase in model membranes. *Biochemistry.* 36:10944–10953.
17. London, E., and D. A. Brown. 2000. Insolubility of lipids in Triton X-100: physical origin and relationship to sphingolipid/cholesterol membrane domains (rafts). *Biochim. Biophys. Acta.* 1508:182–195.
18. Kay, J. G., R. Z. Murray, J. K. Pagan, and J. L. Stow. 2006. Cytokine secretion via cholesterol-rich lipid raft-associated SNAREs at the phagocytic cup. *J. Biol. Chem.* 281:11949–11954.
19. Shogomori, H., A. T. Hammond, A. G. Ostermeyer-Fay, D. J. Barr, G. W. Feigenson, E. London, and D. A. Brown. 2005. Palmitoylation and intracellular domain interactions both contribute to raft targeting of linker for activation of T cells. *J. Biol. Chem.* 280:18931–18942.
20. Umlauf, E., M. Mairhofer, and R. Prohaska. 2006. Characterization of the stomatin domain involved in homo-oligomerization and lipid raft association. *J. Biol. Chem.* 281:23349–23356.
21. Brown, D. A., and E. London. 2000. Structure and function of sphingolipid- and cholesterol-rich membrane rafts. *J. Biol. Chem.* 275: 17221–17224.
22. Fridriksson, E. K., P. A. Shipkova, E. D. Sheets, D. Holowka, B. Baird, and F. W. McLafferty. 1999. Quantitative analysis of phospholipids in functionally important membrane domains from RBL-2H3 mast cells using tandem high-resolution mass spectrometry. *Biochemistry.* 38:8056–8063.
23. Melkonian, K. A., A. G. Ostermeyer, J. Z. Chen, M. G. Roth, and D. A. Brown. 1999. Role of lipid modifications in targeting proteins to detergent-resistant membrane rafts. Many raft proteins are acylated, while few are prenylated. *J. Biol. Chem.* 274:3910–3917.
24. Majerus, P. W., T. M. Connolly, H. Deckmyn, T. S. Ross, T. E. Bross, H. Ishii, V. S. Bansal, and D. B. Wilson. 1986. The metabolism of phosphoinositide-derived messenger molecules. *Science.* 234:1519–1526.

25. Berridge, M. J., and R. F. Irvine. 1989. Inositol phosphates and cell signalling. *Nature*. 341:197–205.
26. Pike, L. J., and J. M. Miller. 1998. Cholesterol depletion delocalizes phosphatidylinositol bisphosphate and inhibits hormone-stimulated phosphatidylinositol turnover. *J. Biol. Chem.* 273:22298–22304.
27. McLaughlin, S., J. Wang, A. Gambhir, and D. Murray. 2002. PIP(2) and proteins: interactions, organization, and information flow. *Annu. Rev. Biophys. Biomol. Struct.* 31:151–175.
28. Hilgemann, D. W., S. Feng, and C. Nasuhoglu. 2001. The complex and intriguing lives of PIP2 with ion channels and transporters. *Sci. STKE.* 2001:RE19.
29. Lopes, C. M., H. Zhang, T. Rohacs, T. Jin, J. Yang, and D. E. Logothetis. 2002. Alterations in conserved Kir channel-PIP2 interactions underlie channelopathies. *Neuron*. 34:933–944.
30. Zhang, L., J. K. Lee, S. A. John, N. Uozumi, and I. Kodama. 2004. Mechanosensitivity of GIRK channels is mediated by protein kinase C-dependent channel-phosphatidylinositol 4,5-bisphosphate interaction. *J. Biol. Chem.* 279:7037–7047.
31. Liu, B., and F. Qin. 2005. Functional control of cold- and menthol-sensitive TRPM8 ion channels by phosphatidylinositol 4,5-bisphosphate. *J. Neurosci.* 25:1674–1681.
32. Martin, T. F. 2001. PI(4,5)P(2) regulation of surface membrane traffic. *Curr. Opin. Cell Biol.* 13:493–499.
33. Czech, M. P. 2003. Dynamics of phosphoinositides in membrane retrieval and insertion. *Annu. Rev. Physiol.* 65:791–815.
34. Yin, H. L., and P. A. Janmey. 2003. Phosphoinositide regulation of the actin cytoskeleton. *Annu. Rev. Physiol.* 65:761–789.
35. Remillard, C. V., and J. X. Yuan. 2006. Transient receptor potential channels and caveolin-1: good friends in tight spaces. *Mol. Pharmacol.* 70:1151–1154.
36. van Rheenen, J., E. M. Achame, H. Janssen, J. Calafat, and K. Jalink. 2005. PIP2 signaling in lipid domains: a critical re-evaluation. *EMBO J.* 24:1664–1673.
37. Shaw, J. E., R. F. Epand, K. Sinnathamby, Z. Li, R. Bittman, R. M. Epand, and C. M. Yap. 2006. Tracking peptide-membrane interactions: insights from in situ coupled confocal-atomic microscopy imaging of NAP-22 peptide insertion and assembly. *J. Struct. Biol.* 155:458–469.
38. Niu, S. L., and B. J. Litman. 2002. Determination of membrane cholesterol partition coefficient using a lipid vesicle-cyclodextrin binary system: effect of phospholipid acyl chain unsaturation and headgroup composition. *Biophys. J.* 83:3408–3415.
39. Silvius, J. R. 2005. Partitioning of membrane molecules between raft and non-raft domains: insights from model-membrane studies. *Biochim. Biophys. Acta.* 1746:193–202.
40. Wang, J., A. Gambhir, G. Hangyas-Mihalyne, D. Murray, U. Golebiewska, and S. McLaughlin. 2002. Lateral sequestration of phosphatidylinositol 4,5-bisphosphate by the basic effector domain of myristoylated alanine-rich C kinase substrate is due to nonspecific electrostatic interactions. *J. Biol. Chem.* 277:34401–34412.
41. Gambhir, A., G. Hangyas-Mihalyne, I. Zaitseva, D. S. Cafiso, J. Wang, D. Murray, S. N. Pentyala, S. O. Smith, and S. McLaughlin. 2004. Electrostatic sequestration of PIP(2) on phospholipid membranes by basic/aromatic regions of proteins. *Biophys. J.* 86:2188–2207.
42. McLaughlin, S., and D. Murray. 2005. Plasma membrane phosphoinositide organization by protein electrostatics. *Nature*. 438:605–611.
43. Golebiewska, U., A. Gambhir, G. Hangyas-Mihalyne, I. Zaitseva, J. Radler, and S. McLaughlin. 2006. Membrane-bound basic peptides sequester multivalent (PIP2), but not monovalent (PS), acidic lipids. *Biophys. J.* 91:588–599.
44. Skene, J. H. P. 1989. Axonal growth-associated proteins. *Annu. Rev. Neurosci.* 12:127–156.
45. Benowitz, L. I., and A. Routtenberg. 1997. GAP-43: an intrinsic determinant of neuronal development and plasticity. *Trends Neurosci.* 20:84–91.
46. Strittmatter, S. M., T. Vartanian, and M. C. Fishman. 1992. GAP-43 as a plasticity protein in neuronal form and repair. *J. Neurobiol.* 23:507–520.
47. Bomze, H. M., K. R. Bulsara, B. J. Iskandar, P. Caroni, and J. H. Skene. 2001. Spinal axon regeneration evoked by replacing two growth cone proteins in adult neurons. *Nat. Neurosci.* 4:38–43.
48. Arni, S., S. A. Keilbaugh, A. G. Ostermeyter, and D. A. Brown. 1998. Association of GAP-43 with detergent-resistant membranes requires two palmitoylated cysteine residues. *J. Biol. Chem.* 273:28478–28485.
49. Skene, J. H. P., and I. Virag. 1989. Posttranslational membrane attachment and dynamic fatty acylation of a neuronal growth cone protein, GAP-43. *J. Cell Biol.* 108:613–624.
50. Buser, C. A., and S. McLaughlin. 1998. Ultracentrifugation techniques for measuring the binding of peptides and proteins to sucrose-loaded phospholipid vesicles. *Methods Mol. Biol.* 84:267–281.
51. Chen, P. S., Jr., T. Y. Toribara, and H. Warner. 1956. Microdetermination of phosphorous. *Anal. Chem.* 28:1756–1758.
52. Quesnel, S., and J. R. Silvius. 1994. Cysteine-containing peptide sequences exhibit facile uncatalyzed transacylation and acyl-CoA-dependent acylation at the lipid bilayer interface. *Biochemistry.* 33: 13340–13348.
53. Gandhavadi, M., D. Allende, A. Vidal, S. A. Simon, and T. J. McIntosh. 2002. Structure, composition, and peptide binding properties of detergent soluble bilayers and detergent resistant rafts. *Biophys. J.* 82:1469–1482.
54. McIntosh, T. J., A. Vidal, and S. A. Simon. 2003. Sorting of lipids and transmembrane peptides between detergent-soluble bilayers and detergent-resistant rafts. *Biophys. J.* 85:1656–1666.
55. Akashi, K.-I., H. Miyata, H. Itoh, and K. Kinosita. 1996. Preparation of giant liposomes in physiological conditions and their characterization under an optical microscope. *Biophys. J.* 71:3242–3250.
56. Fisher, L. D., and G. van Belle. 1993. Biostatistics: A Methodology for Health Sciences. John Wiley and Sons, New York.
57. Pirie, W. R., and M. A. Hamdan. 1972. Some revised continuity corrections for discrete distributions. *Biometrics.* 28:693–701.
58. Kahya, N., D. Scherfeld, K. Bacia, B. Poolman, and P. Schwille. 2003. Probing lipid mobility of raft-exhibiting model membranes by fluorescence correlation spectroscopy. *J. Biol. Chem.* 278:28109–28115.
59. Vidal, A., and T. J. McIntosh. 2005. Transbilayer peptide sorting between raft and nonraft bilayers: comparisons of detergent extraction and confocal microscopy. *Biophys. J.* 89:1102–1108.
60. Shogomori, H., and D. A. Brown. 2003. Use of detergents to study membrane rafts: the good, the bad, and the ugly. *Biol. Chem.* 384:1259–1263.
61. Wilson, B. S., S. L. Steinberg, K. Liederman, J. R. Pfeiffer, Z. Surviladze, J. Zhang, L. E. Samelson, L. H. Yang, P. G. Kotula, and J. M. Oliver. 2004. Markers for detergent-resistant lipid rafts occupy distinct and dynamic domains in native membranes. *Mol. Biol. Cell.* 15:2580–2592.
62. Simons, K., and W. L. Vaz. 2004. Model systems, lipid rafts, and cell membranes. *Annu. Rev. Biophys. Biomol. Struct.* 33:269–295.
63. Lagerholm, B. C., G. E. Weinreb, K. Jacobson, and N. L. Thompson. 2005. Detecting microdomains in intact cell membranes. *Annu. Rev. Phys. Chem.* 56:309–336.
64. Heerklotz, H., H. Szadkowska, T. Anderson, and J. Seelig. 2003. The sensitivity of lipid domains to small perturbations demonstrated by the effect of Triton. *J. Mol. Biol.* 329:793–799.
65. Lichtenberg, D., F. M. Goni, and H. Heerklotz. 2005. Detergent-resistant membranes should not be identified with membrane rafts. *Trends Biochem. Sci.* 30:430–436.
66. Alexander, K. A., B. T. Wakim, G. S. Doyle, K. A. Walsh, and D. R. Storm. 1988. Identification and characterization of the calmodulin-binding domain of neuromodulin, a neurospecific calmodulin-binding protein. *J. Biol. Chem.* 263:7544–7549.
67. Liu, Y. C., and D. R. Storm. 1990. Regulation of free calmodulin levels by neuromodulin: neuron growth and regeneration. *Trends Pharmacol. Sci.* 11:107–111.